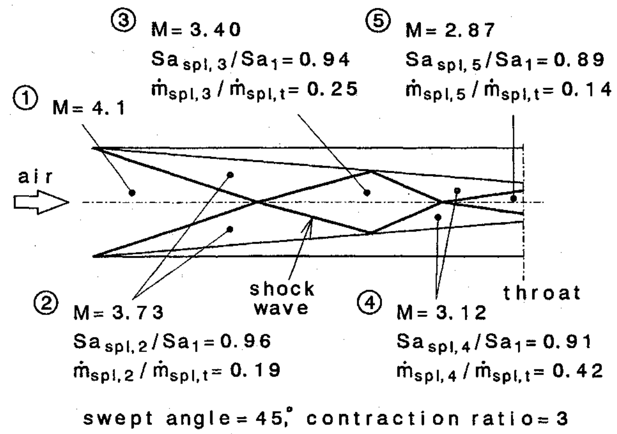

Fig. 3 Stream thrust function in the inlet using the shock-wave relation.

air. The stream thrust function does not change very much with Mach number [see Eq. (3b)]. For example, when a Mach number changes from 10 to 3, the stream thrust function decreases to 0.88 of that of the Mach number of 10. In the preliminary estimation of the engine thrust, the stream thrust function of the spilled air can be estimated as being equal to that of the inflow air. According to the results by Voland,[1] the ratio of the stream thrust function of the spilled air to that of the inflow air was 0.9, and was also around unity.

Figure 3 shows the change of the stream thrust function in the two-dimensional flow of one of the inlets, 45-3(0), calculated using the shock-wave relation. The shock-wave relation was applied to the plane perpendicular to the leading edge of the side wall. The spillage was calculated using the downward component of the velocity and the density after the shock wave, and the area of the specified section. $\dot{m}_{spl,t}$ is the total flow rate of the spilled air. $Sa_{spl,i}$ is the stream thrust function of the spilled air from section i. It does not have the pressure contribution of the second term in Eq. (3a), because the bottom of the side wall was parallel and the plane of the spillage was also parallel to the direction of thrust or drag. The stream thrust function did not change very much near the throat.

As shown in Fig. 2, there was no large change in the pressure drag of the inlet throughout the testing, regardless of whether or not the inlet was in the starting condition. The pressure drag did not increase with the contraction ratio to the degree predicted by the shock-wave relation. The ratio of the spilled air was 0.15 in Fig. 3, while it was 0.25 in the testing. The ratios of the pressure drag, spilled impulse function, and the impulse function of the outflow to the impulse function of the inflow air were 0.10, 0.14, and 0.76, respectively, whereas those in the testing were 0.07, 0.28, and 0.65, respectively. The difference was caused by the spillage caused by the pressure difference between inside and outside the inlet, and because of the end effect of the wall. The pressure difference induces spillage of the downward flow. For example, there is spillage even in the model with no swept angle. Around the top wall, the shock wave from the leading edge of the side wall was rather conical, and the pressure increase across the shock wave was smaller than across the plane shock wave. The disagreement of the calculated values with the experimental results shows the limitation of application of the shock-wave relation for estimation of the drags in the inlet.

Conclusions

The impulse functions and the drag of the side wall compression-type scramjet inlet models were investigated in a Mach 4 flowfield. The following points were clarified:

1) The stream thrust function of the spilled air from the inlet was almost equal to that of the incoming air, and did not change so much with the decrease of the Mach number.

2) The pressure drag of the inlets showed little change, regardless of the model geometry, and regardless of whether or not the inlet was in the starting condition.

Acknowledgment

The authors thank Goro Masuya of Tohoku University for useful discussions.

References

[1]Kanda, T., Komuro, T., Masuya, G., Kudo, K., Murakami, A., Tani, K., Wakamatsu, Y., and Chinzei, N., "Mach 4 Testing of Scramjet Inlet Models," AIAA Paper 89-2680, July 1989.

[2]Voland, R. T., "Methods for Determining the Internal Thrust of Scramjet Engine Modules from Experimental Data," AIAA Paper 90-2340, July 1990.

[3]Vinogradov, V. A., and Stepanov, V. A., "Numerical and Experimental Investigation of Airframe-Integrated Inlet for High Velocities," *Journal of Propulsion and Power*, Vol. 8, No. 1, 1992, pp. 151–157.

[4]Kumar, A., Singh, D. J., and Trexler, C. A., "Numerical Study of the Effect of Reverse Sweep on Scramjet Inlet Performance," *Journal of Propulsion and Power*, Vol. 8, No. 3, 1992, pp. 714–720.

[5]White, F. M., "Viscous Fluid Flow," McGraw–Hill, New York, 1974, pp. 632–640.

[6]Heiser, W. H., and Pratt, D. T., *Hypersonic Airbreathing Propulsion*, AIAA Education Series, AIAA, Washington, DC, 1994, p. 63.

Hollow Projectile Operation in the Ram Accelerator

A. Sasoh,* A. J. Higgins,† C. Knowlen,‡ and A. P. Bruckner§

University of Washington, Seattle, Washington 98195-2250

Introduction

THE ram accelerator is a chemically energized mass driver that has the potential for launching heavy payloads at high speeds.[1] In this device, a subcaliber projectile is injected at supersonic speed into a tube filled with pressurized combustible gas mixtures. Combustion is initiated by the passage of the projectile that results in a pressure field that continuously accelerates it. Applications of this technology include direct space launch, hypersonic ground test facilities, a research tool to study supersonic reactive flow phenomena, and hypervelocity impact experiments. To realize these applications, the operational characteristics of the ram accelerator need to be better understood.

Currently, the experimental diagnostics of the flowfield in a ram accelerator are limited to measurements made at the tube

Received Oct. 4, 1995; revision received May 28, 1996; accepted for publication June 9, 1996.

*Visiting Scholar, Aerospace and Energetics Research Program; currently Associate Professor, Shock Wave Research Center, Institute of Fluid Science, Tohoku University, 2-1-1 Katahira, Aoba-ku, Sendai 980-77, Japan. Member AIAA.

†Graduate Student, Aerospace and Energetics Research Program. Student Member AIAA.

‡Research Scientist, Aerospace and Energetics Research Program. Member AIAA.

§Professor, Aerospace and Energetics Research Program. Associate Fellow AIAA.

wall. With a conventional centerbody projectile, resulting from the existence of centering fins, the reactive flowfield is three dimensional, requiring high instrumentation density for adequate spatial resolution.[2] Simplification of the flowfield would significantly increase the understanding of the related phenomena. One possible approach is to obtain axisymmetric flow by using a hollow projectile; i.e., a cylinder bored out to provide an area profile similar to that of a centerbody projectile. The results from an experimental investigation using such projectiles are presented here.

Experimental Apparatus

The experiments were conducted using the 38.1-mm-bore ram accelerator facility at the University of Washington.[1,3] In this study, only 8 m of the 16-m-long ram accelerator test section was used. The projectiles were saboted with the same obturator used for the centerbody projectiles and launched by a helium gas gun to speeds ranging from 1000 to 1200 m/s. The velocity and acceleration were determined from the time–distance data collected by electromagnetic sensors spaced at 0.4-m intervals. The pressure histories on the tube were measured by piezoelectric transducers (PCB 119M44), and combustion luminosity was monitored with optical fibers and photodiodes. The initial pressure of the ram accelerator test section was 2.5 MPa.

The hollow projectiles used in this study, shown in Fig. 1, were made of 7075-T6 aluminum alloy. The o.d. is 38.0 mm, which is 0.1 mm smaller than the tube bore. The projectiles have a 10-deg inverse cone diffuser. To avoid damage from the penetration of the Mylar diaphragms in the facility, the apex angle of the diffuser lip was increased to 30 deg. The cross-sectional throat-to-tube area ratio is 0.41, equaling that of a conventional centerbody projectile.[1-5] The downstream section is a diverging inverse cone, truncated by a flat base. The cross-sectional area ratio of the flow passage at the base also equals that of the conventional projectile (with fins being taken into account). An annular magnet is installed into the groove on the side of the projectiles. The masses of type A and B projectiles are 0.105 and 0.095 kg, respectively.

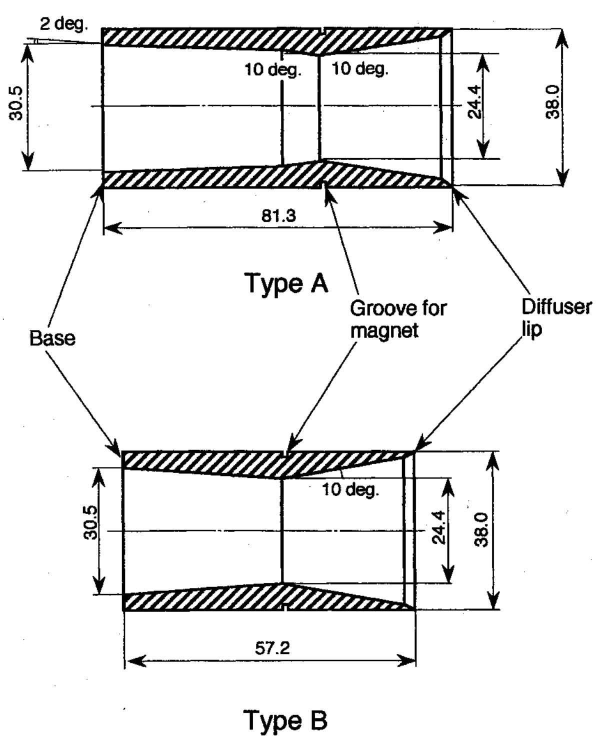

Fig. 1 Hollow ram accelerator projectiles, dimensions in mm.

Results and Discussion

A series of inert firing into $CH_4-N_2-CO_2$ mixtures was conducted to determine the minimum entrance Mach number that would allow the projectile to be separated from the sabot while maintaining supersonic flow through its interior. This turned out to be M_{p0} (entrance Mach number) ~ 3.4 for the hollow projectiles, which is ~30% higher than that determined for centerbody projectiles.[4] In the case of the hollow projectiles, the total pressure loss arising from the inverse conical diffuser is large; an estimation of the minimum entrance Mach number made by assuming isentropic flow is not accurate. Since the prelauncher limited the entrance velocity to 1200 m/s, this constrained the maximum allowable acoustic speed of the propellant mixture. This requirement was met by using a propellant mixture composed of $XCH_4 + 2O_2 + YCO_2$ (X = 1.5 or 2.8, Y = 2.5–4.5), which has acoustic speeds ranging from 302–330 m/s.

Once a normal shock wave disgorges upstream of the diffuser's throat, flow at the diffuser inlet of the projectile becomes subsonic and the projectile experiences large deceleration. This operation failure will hereafter be referred to as an unstart. There are mainly three causes for unstart.

1) One is because of a strong shock wave generated by the heat release of combustion (combustion unstart).

2) Another is because of the failure of quasi-steady-state supersonic diffuser operation, which can occur without the heat release (gasdynamic unstart).

3) The other is because of structural failure of the projectile.

Examination of the projectiles after the firings revealed that the structural failure did not occur in this investigation.

The primary variables considered in this investigation were propellant energetics, entrance velocity, and projectile geometry. The experimental parameters and corresponding results are listed in Table 1. The first three experiments (nos. 1–3) explored the effect of propellant energetics on the ignition process for the type A projectile at an entrance Mach number of about 3.6. The velocity–distance data from these firings are shown in Fig. 2. It was found that varying the CO_2 concentration from 34 to 45% (Y = 2.5–4.0) would change the experimental result from immediate combustion unstart (Y = 2.5) to no ignition (Y = 4.0). In the latter case the projectile decelerated supersonically until gasdynamic unstart at M_{p0} = 2.8, which is higher than the M_{p0} = 2.3 predicted for an isentropic diffuser having the same area ratio.

The type A projectile was accelerated for 2.6 m of the test section in the X = 2.8, Y = 3.0 propellant mixture (no. 2, Table 1) with a velocity gain of 108 m/s (Fig. 2). The pressure–time data of this experiment are shown in Fig. 3 along with the luminosity data from a station located 1.8 m from the entrance to the test section. Upon ignition, the pressure at the base of the projectile was about 30 MPa and the intensity of the luminosity peaked downstream of the projectile. This implies that the majority of the combustion was occurring behind the

Table 1 Experimental parameters and results of hollow projectile firings[a]

No.	X	Y	Projectile	U_{p0}, m/s	M_{p0}	ΔU_p, m/s
1	2.8	2.5	A	1160	3.5	Immediate CU[b]
2	2.8	3.0	A	1166	3.6	108
3	2.8	4.0	A	1162	3.7	No ignition
4	1.5	4.5	A	1163	3.9	15
5	1.5	4.5	B	1013	3.4	No ignition
6	1.5	4.5	B	1090	3.6	59
7	1.5	4.5	B	1177	3.9	71
8	1.5	4.0	B	1020	3.4	67
9	1.5	4.0	B	1088	3.6	44
10	1.5	4.0	B	1184	3.9	Immediate CU[b]
11	2.8	3.0	B	1174	3.6	62

[a] $XCH_4 + 2O_2 + YCO_2$, p_1 = 2.5 MPa. [b] CU, combustion unstart.

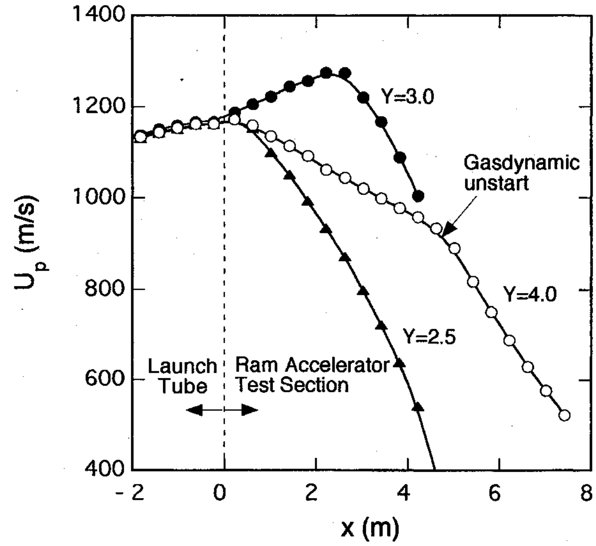

Fig. 2 U_p **(projectile velocity) vs** x **(distance from entrance diaphragm), nos. 1–3 in Table 1,** $2.8CH_4 + 2O_2 + YCO_2$**. Error in measuring** U_p **is ±6 m/s.**

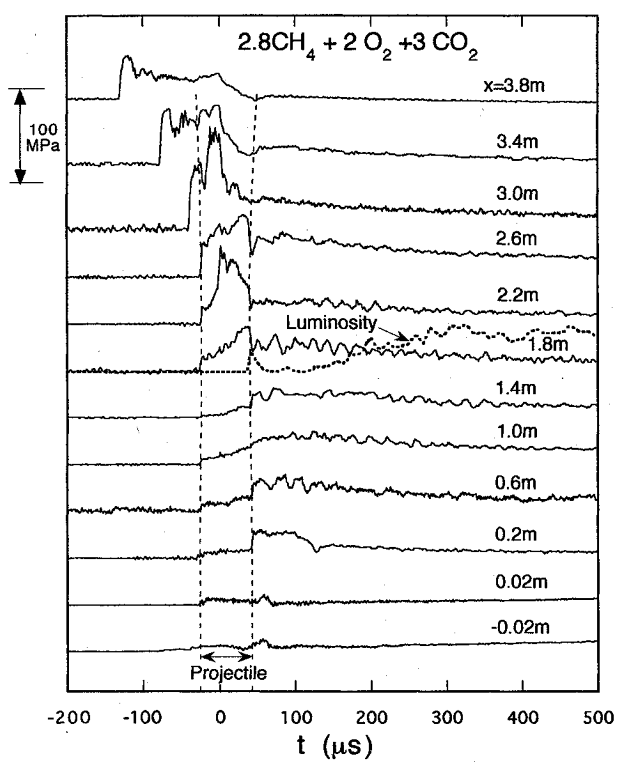

Fig. 3 Pressure histories, $X = 2.8$**,** $Y = 3.0$**, no. 2 in Table 1,** $t = 0$ **corresponds to the throat location. Luminosity (in an arbitrary unit) at** $x = 1.8$ **m is also plotted by a broken line.**

projectile. After 2.6 m of ram acceleration, the projectile experienced a combustion unstart, as indicated by the shock wave propagating ahead of the projectile ($X \geq 3.0$ m). The results of these three experiments have shown that, with respect to propellant energetics, there is a relatively small operation envelope for the hollow projectile.[5]

The effects of entrance velocity were investigated with type B projectiles in a propellant mixture having $X = 1.5$ and $Y = 4.0$ or 4.5 (nos. 5–10, Table 1). No ignition was observed at an entrance velocity of 1013 m/s ($M_{p0} = 3.4$) in the $Y = 4.5$ propellant mixture; however, ram acceleration was established when the entrance velocity was increased to 1090 ($M_{p0} = 3.6$) to 1177 m/s ($M_{p0} = 3.9$). Increasing the propellant energetics slightly by reducing the CO_2 concentration by 3% ($Y = 4.0$) resulted in successful projectile acceleration at 1020 m/s ($M_{p0} = 3.4$), but an immediate combustion unstart at 1184 m/s ($M_{p0} = 3.9$). Thus, a range of entrance velocities, which are sensitive to diluent concentration, has been established in which ram acceleration can be achieved.

Type A and B projectiles were fired into two different propellant mixtures at an entrance velocity of about 1170 m/s (nos. 2, 4, 7, and 11, Table 1). In the $X = 2.8$, $Y = 3.0$ propellant mixture, the largest velocity gain was realized with type A. However, in the $X = 1.5$, $Y = 4.5$ propellant mixture, type B had a larger velocity gain. Thus, the effects of the projectile geometry were not conclusively determined from these experiments.

For the thermally choked ram accelerator propulsion mode,[1,3] the nondimensional thrust $F/(p_1A_t)$ (A_t, tube cross-sectional area; F, thrust; p_1, initial tube pressure) should decrease from 3.5 to 2.7 as the projectile velocity increases from $U_{p0} = 1170$ to 1270 m/s for the experimental condition of no. 2 in Table 1. However, the mean value of the measured nondimensional thrust is 1.9, much smaller than the theoretical value. Using a thin wall approximation, the expansion of the hollow projectile o.d. is estimated by $\Delta D = pD^2/(2tE)$ (D, outer diameter; E, Young's modulus; p, pressure; t, effective wall thickness). Inputting typical values at the base of the projectile, $D = 38.0$ mm, $E = 7.2 \times 10^{10}$ Pa, $p = 3 \times 10^7$ Pa, $t = 3.75$ mm, ΔD is calculated to be 0.08 mm, comparable with the clearance, 0.1 mm. Considering uncertainties in this estimation of the pressure distribution, the temperature dependence of material strength, etc., it is expected that under high-pressure ΔD can exceed the clearance, and the friction force of the projectile against the tube wall resulting from this expansion can be significant. Moreover, flow through the small gap between the projectile and the tube wall is equivalent to Couette flow, in which the effect of viscosity is large; the static temperature increases and the mixture may be ignited there. The effect of gap clearance warrants further investigation.

Summary

In this study, positive acceleration was obtained with hollow projectiles; however, the velocity gains were modest (~100 m/s), and the projectiles failed to accelerate for more than 3 m. These results indicate that further studies are required to enhance hollow projectile performance in the ram accelerator. The phenomena limiting the operating velocity range are believed to be gasdynamic and structural. The gasdynamic problems are based on the fact that with the same apex angle, a shock wave generated at the leading edge is stronger for a hollow projectile than for a centerbody projectile. This makes the operational velocity range and chemistry regime for the hollow projectiles relatively narrow. Thus, the mixture and the entry speed must be appropriately matched. In addition, the projectile tip must be carefully designed, both to keep the shock wave weak enough to allow for proper diffuser operation and to maintain the integrity of the leading edge during diaphragm rupture. The structural problem derives from the expansion of projectile diameter caused by the high pressures inside. This effect may cause excessive frictional drag on the wall.

Acknowledgments

This work was supported in part by a cooperative science program sponsored by the National Science Foundation and the Japan Society for Promotion of Science. The help of G. Chew in designing the hollow projectiles through computational fluid dynamics and the assistance provided by T. Imrich and J. Elvander in the experiments are greatly appreciated. We are also grateful for the efforts of M. Saynor and D. Peterson in machining the projectiles. Finally, the authors would like to express their appreciation of the valuable suggestions made by A. Hertzberg.

References

[1]Hertzberg, A., Bruckner, A. P., and Bogdanoff, D. W., "Ram Accelerator: A New Chemical Method for Accelerating Projectiles to Ultrahigh Velocities," *AIAA Journal*, Vol. 26, No. 1, 1988, pp. 195–203.

[2]Hinkey, J. B., Burnham, E. A., and Bruckner, A. P., "High Spatial Resolution Measurements of Ram Accelerator Gas Dynamic Phenomena," AIAA Paper 92-3244, July 1992.

[3]Bruckner, A. P., Knowlen, C., Hertzberg, A., and Bogdanoff, D. W., "Operational Characteristics of the Thermally Choked Ram Accelerator," *Journal of Propulsion and Power*, Vol. 7, No. 5, 1991, pp. 828–836.

[4]Burnham, E., "Investigation of Starting and Ignition Transients in the Thermally Choked Ram Accelerator," Ph.D. Disstation, Univ. of Washington, St. Louis, MO, Dec. 1993.

[5]Knowlen, C., Higgins, A. J., and Bruckner, A. P., "Investigation of Operational Limits to the Ram Accelerator," AIAA Paper 94-2967, June 1994.